AGU PUBLICATIONS

Water Resources Research

RESEARCH ARTICLE
10.1002/2017WR020551

Processes governing arsenic retardation on Pleistocene sediments: Adsorption experiments and model-based analysis

Bhasker Rathi[1,2], Harald Neidhardt[3], Michael Berg[4], Adam Siade[1,5], and Henning Prommer[1,2,5]

[1]School of Earth Sciences, University of Western Australia, Nedlands, Western Australia, Australia, [2]CSIRO Land and Water, Wembley, Western Australia, Australia, [3]Department of Geosciences, University of Tübingen, Tübingen, Germany, [4]Eawag, Swiss Federal Institute of Aquatic Science and Technology, Dübendorf, Switzerland, [5]National Centre for Groundwater Research and Training, Adelaide, South Australia, Australia

Key Points:
- Arsenite, As(III), sorption onto natural Pleistocene sediments is controlled by primary (adsorption) and secondary (oxidation) processes
- Geochemical modeling framework improves interpretation of the analytical data and shows importance of coupling between the two processes
- 1-D reactive transport simulations show significant impact of available sorption sites, As(III) and PO_4 concentrations on arsenic retardation

Supporting Information:
- Supporting Information S1
- Figure S1
- Figure S2

Correspondence to:
H. Prommer,
henning.prommer@csiro.au

Citation:
Rathi, B., H. Neidhardt, M. Berg, A. Siade, and H. Prommer (2017), Processes governing arsenic retardation on Pleistocene sediments: Adsorption experiments and model-based analysis, *Water Resour. Res.*, *53*, 4344–4360, doi:10.1002/2017WR020551.

Received 9 FEB 2017
Accepted 2 MAY 2017
Accepted article online 8 MAY 2017
Published online 31 MAY 2017

Abstract In many countries of south/south-east Asia, reliance on Pleistocene aquifers for the supply of low-arsenic groundwater has created the risk of inducing migration of high-arsenic groundwater from adjacent Holocene aquifers. Adsorption of arsenic onto mineral surfaces of Pleistocene sediments is an effective attenuation mechanism. However, little is known about the sorption under anoxic conditions, in particular the behavior of arsenite. We report the results of anoxic batch experiments investigating arsenite (1–25 μmol/L) adsorption onto Pleistocene sediments under a range of field-relevant conditions. The sorption of arsenite was nonlinear and decreased with increasing phosphate concentrations (3–60 μmol/L) while pH (range 6–8) had no effect on total arsenic sorption. To simulate the sorption experiments, we developed surface complexation models of varying complexity. The simulated concentrations of arsenite, arsenate, and phosphate were in good agreement for the isotherm and phosphate experiments while secondary geochemical processes affected the pH experiments. For the latter, the model-based analysis suggests that the formation of solution complexes between organic buffers and Mn(II) ions promoted the oxidation of arsenite involving naturally occurring Mn-oxides. Upscaling the batch experiment model to a reactive transport model for Pleistocene aquifers demonstrates strong arsenic retardation and could have useful implications in the management of arsenic-free Pleistocene aquifers.

1. Introduction

Arsenic contamination in the south/south-east (S/SE) Asian region affects the health of millions of individuals who rely on groundwater as the main source for drinking and irrigation water [*Smedley and Kinniburgh*, 2002]. Elevated arsenic levels are common in the groundwater sourced from the Holocene aquifers in this region, while, on the other hand, groundwater extracted from the Pleistocene aquifers is characteristically low in arsenic (<10 μg/L) [*Fendorf et al.*, 2010]. Therefore, the reliance on groundwater extraction from Pleistocene aquifers has been rapidly increasing over the past few decades. This has raised considerable concerns over the long-term sustainability of these aquifers due to the alteration in the local and regional hydrology in some areas [*van Geen et al.*, 2013], thereby inducing the migration of high-arsenic groundwater both, laterally and vertically, into Pleistocene aquifers and threatening the supply wells [*Berg et al.*, 2008; *Fendorf et al.*, 2010; *Harvey et al.*, 2002; *Winkel et al.*, 2011].

The long-term sustainability of Pleistocene aquifers requires both hydrological and geochemical protection from arsenic migration [*McArthur et al.*, 2008; *Stollenwerk*, 2003; *Stute et al.*, 2007]. In the absence of a confining layer between Holocene and Pleistocene aquifers, hydrological protection would occur in cases where the recharge area of an aquifer has low dissolved arsenic concentrations and the solutes, such as dissolved organic carbon (DOC) that can mobilize arsenic, are absent [*Burgess et al.*, 2010]. Achieving sustainability solely on the basis of hydrological protection strategies would require different approaches for shallow local groundwater sources compared to deeper regional aquifers. *Michael and Voss* [2008], for example, have illustrated through large-scale numerical modeling that specific pumping strategies might be able to provide low-arsenic water from Pleistocene aquifers for domestic and irrigation use.

The role of geochemical protection relies largely on two specific arsenic attenuation mechanisms, namely, adsorption and precipitation [*Fendorf et al*., 2010]. Among the latter, secondary arsenic sulfide precipitation is the most widely recognized mechanism in reducing aquifers [*Lowers et al*., 2007]. However, studies of arsenic mobility under sulfate-reducing conditions have shown that sulfide production can lead to the formation of thioarsenic species, which is known to significantly enhance arsenic mobility [*Planer-Friedrich et al*., 2007]. Therefore, arsenic adsorption onto sediments will in many cases be the most reliable process for attenuating dissolved arsenic concentrations in groundwater. However, a significant knowledge gap still exists with respect to quantitative studies of arsenic adsorption onto natural aquifer sediments. Such studies are extremely important to develop and implement reliable management strategies for vulnerable aquifers in S/SE Asia.

A number of modeling approaches have been suggested in the literature for quantification of sorption processes. Despite its well-known shortcomings, the distribution coefficient (K_d) approach is still the most widely used concept for quantifying arsenic adsorption in both laboratory and field-scale numerical models [*Radloff et al*., 2011; *van Geen et al*., 2013; *Zhang and Selim*, 2005]. The K_d approach often fails to represent both the spatially and temporally varying geochemical conditions and the associated variations in the partitioning behavior between the aqueous and sorbed phases of the contaminant [*Tessier et al*., 1989]. However, surface complexation models (SCMs) can explicitly consider this variability, and a wide range of SCMs have been developed and applied for both metals and metalloids, including arsenic [*Biswas et al*., 2014; *Jessen et al*., 2012; *Jung et al*., 2009; *Rawson et al*., 2016; *Stollenwerk et al*., 2007]. SCMs provide a process-based quantification of arsenic adsorption behavior as a function of varying arsenic solution concentration, arsenic speciation, and solution pH. SCMs also consider the influence of competing ions such as phosphate or bicarbonate, as well as the density of adsorption sites on host minerals, such as Fe-oxides. However, several shortcomings in the existing SCMs for arsenic limit their wider application, including the application to Pleistocene aquifers in S/SE Asia. First, most of the SCMs have been developed for pure, synthetic minerals, e.g., Fe-oxides and Al-oxides [*Dixit and Hering*, 2003; *Dzombak and Morel*, 1990; *Karamalidis and Dzombak*, 2010; *Stachowicz et al*., 2008], while natural sediments consist of an aggregate of different minerals for which the combined surface properties are not comparable to those of single synthetic minerals [*Davis and Kent*, 1990; *Davis et al*., 1998]. Second, the few attempts to construct SCMs for Pleistocene sediments were all using data from adsorption experiments that were performed with arsenate (As(V)) [e.g., *Stollenwerk et al*., 2007]. This was justified based on the assumption that arsenite (As(III)) would be oxidized upon contact with Pleistocene sediments [*Stollenwerk et al*., 2007] or by assuming that the adsorption behavior of As(III) and As(V) at near-neutral pH conditions was similar [*Robinson et al*., 2011]. However, both assumptions are controversial as the As(III) oxidation during the migration from Holocene into Pleistocene aquifer sections has been disputed [*Radloff et al*., 2011; *Thi Hoa Mai et al*., 2014] along with clearly contrasting adsorption characteristics of As(III) and As(V) for Red River floodplain sediments [*Thi Hoa Mai et al*., 2014].

Therefore, this study is aimed at providing characterization and model-based quantification of As(III) adsorption behavior onto natural Pleistocene sediments, typical of S/SE Asia, under varying geochemical conditions. The sediments were obtained from a well-characterized field site in Vietnam which represents typical conditions of arsenic polluted Pleistocene aquifers in S/SE Asia [*Berg et al*., 2008]. We used these sediments for laboratory batch adsorption experiments and analyzed the data using a nonelectrostatic generalized composite-surface complexation model (GC-SCM) [*Davis et al*., 1998]. Secondary geochemical processes were considered in the model simulations to investigate the magnitude of their impact on experimental results.

2. Methods

2.1. Study Site

The study site from which the Pleistocene sediments were collected is located in the village of Van Phuc, 10 km south-east of Hanoi on the banks of the Red River, Vietnam. Research into arsenic has been conducted at this site for more than 10 years [*Berg et al*., 2008]. The aquifers at Van Phuc are shallow, and the lateral depositions of Holocene and Pleistocene sediments are generally not hydraulically separated by an

aquitard [*Stahl et al*., 2016]. Similar to the situation in many delta regions of S/SE Asia, reductive dissolution of Fe-oxide minerals in the younger Holocene depositions at Van Phuc has resulted in the natural enrichment of arsenic in groundwater [*Berg et al*., 2008]. Steadily increasing pumping for the water supply of Hanoi City for over 100 years [*Winkel et al*., 2011] has caused a reversal of the natural hydraulic head gradient at Van Phuc, causing groundwater to flow from the river toward Hanoi. This flow reversal has resulted in the migration of arsenic contaminated groundwater from Holocene sediments into previously uncontaminated Pleistocene sediments [*van Geen et al*., 2013].

2.1.1. Sediment Material

The Pleistocene sediment material used in our experiments was obtained in April 2006 during a previously reported field study [*Eiche*, 2009; *Eiche et al*., 2010, 2008]. The particulars of sample collection and storage procedures are provided in supporting information. The results of various mineral analyses on fresh sediment material confirmed it to be oxidized (Fe(III)-oxides content 4.1 wt %), typical of Pleistocene sediments found in the S/SE Asian alluvial systems and the amount of presorbed arsenic, presumably As(V), was measured to be 4.0 μmol/kg of the sediment. The total organic carbon content in the sediment material was measured to be 0.03% by weight and was considered to have low reactivity based on the $\delta^{13}C$ signature data and high C/N ratios [*Eiche*, 2009; *Eiche et al*., 2008]. Prior to using the sediment material in our study, there were no indications of significant alterations in its properties. The specific surface area of the sediment was 3.52 ± 0.18 m^2/g determined by the Brunauer-Emmett-Teller (BET) N_2 gas adsorption method on a Coulter SA3100 surface area analyzer. The original sediment material contained no gravel (>2 mm) [*Eiche*, 2009] and was sieved to a grain size of <0.5 mm for use in our experiments. The sieving was believed to have a minimal effect on the overall mineral composition of the sediment.

2.2. Adsorption Experiments

A series of laboratory experiments were performed to characterize As(III) sorption behavior on Pleistocene sediments using solutions with compositions representative of Holocene groundwater. These experiments were designed to examine As(III) adsorption behavior on Pleistocene sediments with varying As(III) concentrations, solution pH and PO_4 concentrations. These experiments were conducted in anaerobic conditions to simulate the geochemical conditions typical of Pleistocene and Holocene aquifers in S/SE Asia.

The sorption experiments were conducted in batch reactors, each containing 1.00 g of sediment material and 25 mL of 15 mmol/L NaCl (Sigma Aldrich, ≥99.0%) solution. The NaCl solution ionic strength was representative of typical Holocene groundwater at the Van Phuc site and was deoxygenated by purging with argon gas for 3 h. The deoxygenated solution was moved inside an anaerobic chamber (MBRAUN UNIlab Plus, N_2 99.999%, $O_2 < 1$ ppm) and no dissolved O_2 was detected (Hach HQ40d meter/LDO sensor).

The stock solutions of As(III) and inorganic phosphate (PO_4) were prepared freshly before each experiment from analytical grade sodium (meta)arsenite (90%, Sigma Aldrich) and $Na_2HPO_4.2H_2O$ (Merck, ≥98.0%). Any adjustments to the solution pH were carried out with 10 mmol/L organic buffers MES (2-(*N*-morpholino) ethanesulfonic acid, Sigma, ≥99.0%) or MOPS (3-(*N*-morpholino)propanesulfonic acid, Fluka, ≥99.0%). Additionally, an artificial groundwater (AGW) solution similar to the average composition of Holocene groundwater at the Van Phuc site was prepared in CO_2 purged deionized water by adding NaCl (Sigma Aldrich, ≥99.0%), $FeCl_2$ (Sigma, ≥98.0%), $MnCl_2.4H_2O$ (Fluka, ≥99.0%), $CaCO_3$ (Merck, ≥99.0%), $K_2HPO_4.3H_2O$ (Merck, ≥99.0%), K_2CO_3 (Merck, ≥99.0%), and MgO (Merck, ≥97.0%). The chemical composition of the AGW is listed in Table 1.

Table 1. Chemical Composition of AGW Solution

Solution Species	Concentrations
Na	0.30 mmol/L
Cl	0.68 mmol/L
K[a]	4.20 mmol/L
Mg	1.39 mmol/L
Ca	2.25 mmol/L
PO_4	22.60 μmol/L
Mn(II)	1.64 μmol/L
Fe(II)	0.19 mmol/L
TCO_2[b]	11.47 mmol/L

[a]Solution potassium (K) concentration was computed from the charge balance calculation in PHREEQC.
[b]Measured using titration method with MColortest™ Alkalinity test kit.

Samples were prepared in amber glass vials to prevent photocatalyzed oxidation of As(III). The batch experiments and solution extractions were carried out in the dark and under N_2 atmosphere within the anaerobic chamber at 25°C. The solution pH was measured at the end of each experiment (IQ125 miniLab Professional pH meter) and sample solutions were filtered to 0.2 μm through nylon membrane syringe filters (Whatman). A 6 mL aliquot from each filtered solution was separated

using a disposable aluminosilicate cartridge [*Meng and Wang*, 1998], at a flow rate of approximately 6 mL/min, for aqueous arsenic speciation. Out of the remaining sample filtrates, 10 mL of each was used for measuring the concentrations of total dissolved arsenic, PO_4 and other solutes. The filtered samples were acidified with ultrapure HNO_3 (Sigma Aldrich) for preservation and stored under 4°C. The amount of adsorbed As(III) in the experiments was determined by difference between initial and final aqueous concentrations.

A series of preliminary experiments were conducted to understand the rate of As(III) adsorption onto Pleistocene sediments. Based on the results of these tests, a duration of 7 days was selected to be the most appropriate for the main adsorption experiments (see supporting information Figure S1). The first set of main adsorption experiments was conducted to determine the concentration-dependent adsorption of As(III) to the sediment through an adsorption isotherm. A total of 11 samples, in triplicate, were used with initial As(III) concentrations ranging from 0.1 to 25 μmol/L and at the natural sediment suspension pH. An adsorption isotherm for As(III) was also determined for seven samples, in duplicate, containing sediment suspension in the AGW solution.

In another set of experiments, the competition effect between As(III) and PO_4 was studied for three initial As(III) concentrations—1, 2.5, and 7.5 μmol/L, and for PO_4 concentrations ranging from 3 to 60 μmol/L in a total of 15 samples, in duplicate. These concentration ranges are characteristically similar to the average composition of Holocene groundwater in S/SE Asia.

In the final set of experiments, the pH effect on As(III) adsorption was studied for two initial As(III) concentrations—1 and 7.5 μmol/L, at six different pH values representing the range typically found in the Holocene groundwater of S/SE Asia, including Van Phuc. The experiment was conducted on a total of 12 samples, in duplicate, with the solution pH modified to 6.1 and 6.5 (using MES buffer), and to 6.8, 7.2, 7.5, and 7.9 (using MOPS buffer). The dissolved solute concentrations in all extracted sample solutions were measured using ICP-MS (Agilent 7500cx).

2.3. Geochemical Modeling

2.3.1. Modeling Approach and Tools

The data collected from the experiments were analyzed using the geochemical modeling code PHREEQC version 2 [*Parkhurst and Appelo*, 1999]. The primary objective of the model simulations was to develop a process-based quantitative description of the arsenic adsorption behavior on the Van Phuc Pleistocene sediments, which could potentially be applied to other study sites with similar geochemical characteristics. A PHREEQC model was constructed to simulate the experimental response for each of the 45 samples using stepwise batch-type reactions between the solution and sediment surface. The thermodynamic data for the relevant aqueous species in the model are included in supporting information. A nonelectrostatic GC-SCM was used to simulate surface complexation reactions as it was better suited to the inherent physical and chemical heterogeneity of the sediment material [*Davis et al*., 1998]. The model construction was based on the geochemical conceptualization of the processes occurring in the experiments, which contained a significant degree of uncertainty. Therefore, conceptual models of different complexity were formulated and their suitability to describe the experimental data was assessed (Table 2). Where available, measured properties, such as initial aqueous solution concentrations, were used as model inputs, and parameters were estimated through a joint inversion procedure in which measured concentrations were used for model calibration.

Table 2. Conceptual Models, Included Reaction Processes and Assumptions

	Primary (Surface Complexation) Reactions		Assumptions for Presorbed As(V)		Secondary Reactions		
Model	As(III) and PO_4 on Site Vp_*a* As(V) and PO_4 on Site Vp_*b*	Mn(II) on Site Mn_*c*	Fixed (4.0 μmol As/kg Sediment) (Ref *a*)[a]	Unknown (Estimated)	None	Organic Buffer and Mn^{2+} Solution Complex	Kinetically Controlled As(III) Oxidation by Mn-Oxides
M1 (refer to section 3.2.1)	✓	✗	✓	✗	✓	✗	✗
M2 (refer to section 3.2.2)	✓	✗	✗	✓	✓	✗	✗
M3 (refer to section 3.3.3)	✓	✓	✗	✓	✗	✓	✓

[a]Ref *a*: *Eiche* [2009] and *Eiche et al*. [2008].

2.3.2. Model Calibration

The parameter estimation procedure for the various conceptual models of different complexity included up to 29 parameters (Table 3) and 160 observations. The number of moles of each surface site (m) and the logarithmic value of the apparent equilibrium constant (log K) of each surface complexation reaction were included in the list of all model parameters that were estimated during the calibration procedure. The observations consisted of measured concentrations of As(III), total arsenic, PO_4, and Mn(II). The sum of squared residuals between measured and modeled data was used as the objective function, and subsequently minimized during the calibration process.

The models considered in this study result in inverse problems that are in general highly nonlinear. Commonly used SCM calibration tools, e.g., FITEQL [*Herberlin and Westall*, 1999], UCODE [*Poeter and Hill*, 1999], or PEST [*Doherty*, 2010], were deemed potentially unreliable in producing a global solution because the objective surface can be highly nonconvex [*Abdelaziz and Zambrano-Bigiarini*, 2014; *Goldberg*, 1991; *Yeh*, 1986]. In fact, in this study, we initially attempted to use the Gauss-Levenberg-Marquardt (GLM) algorithm contained in PEST, and found that it was susceptible to falling into local minima, and alone could not yield well-calibrated models. Therefore, heuristic, global-search methodologies were explored, and Particle Swarm Optimization (PSO) was chosen for this study [*Coello et al*., 2004; *Eberhart and Kennedy*, 1995; *Kennedy et al*., 2001]. A PSO code was written within the PEST++ YAMR run manager [*Welter et al*., 2015], and linked with PHREEQC for the estimation of parameters, similar to the study conducted by *Rawson et al*. [2016]. To further improve the calibration, the GLM algorithm was employed to conduct a local search in the neighborhood of the parameter set resulting from PSO calibration. Tikhonov regularization [*Tikhonov and Arsenin*, 1977] was also employed during this secondary calibration step to incorporate prior information from *Stollenwerk et al*. [2007], remediating the potential impacts of overparameterization, or overfitting.

Table 3. Modeled Reaction Network and Estimated Parameters

Surface Site	Solution Species	Reactions	Parameters	Values for Model M1 (Section 3.2.1)	M2 (Section 3.2.2)	M3 (Section 3.3.3)	*Stollenwerk et al*. [2007]
Vp_*a*	H^+ and OH^-	1. Vp_*a* $OH + H^+ = Vp\_a\,OH_2^+$	pK_a^1	2.10	3.14	3.80	
		2. Vp_*a* $OH = Vp\_a\,O^- + H^+$	pK_a^2	−2.96	−3.21	2.76	
	As(III)	3. Vp_*a* $OH + AsO_3^{3-} + 3H^+ = Vp\_a\,H_2AsO_3 + H_2O$	log K_a^1	42.75	45.02	42.02	37.50
		4. Vp_*a* $OH + AsO_3^{3-} + 2H^+ = Vp\_a\,HAsO_3^- + H_2O$	log K_a^2	42.31	42.09	42.29	32.10
		5. Vp_*a* $OH + AsO_3^{3-} + H^+ = Vp\_a\,AsO_3^{2-} + H_2O$	log K_a^3	33.41	27.63	26.21	30.01
	PO_4	6. Vp_*a* $OH + PO_4^{3-} + 3H^+ = Vp\_a\,H_2PO_4 + H_2O$	log K_a^4	30.10	30.66	34.98	
		7. Vp_*a* $OH + PO_4^{3-} + 2H^+ = Vp\_a\,HPO_4^- + H_2O$	log K_a^5	28.84	28.55	28.74	
		8. Vp_*a* $OH + PO_4^{3-} + H^+ = Vp\_a\,PO_4^{2-} + H_2O$	log K_a^6	20.95	21.02	11.87	
		Surface sorption site (moles)	m_a	1.108×10^{-5}	1.065×10^{-5}	1.302×10^{-5}	
Vp_*b*	H^+ and OH^-	9. Vp_*b* $OH + H^+ = Vp\_b\,OH_2^+$	pK_b^1	3.13	1.94	5.48	7.43
		10. Vp_*b* $OH = Vp\_b\,O^- + H^+$	pK_b^2	−6.40	−6.42	−7.05	−7.03
	As(V)	11. Vp_*b* $OH + AsO_4^{3-} + 3H^+ = Vp\_b\,H_2AsO_4 + H_2O$	log K_b^1	31.03	27.85	27.99	30.66
		12. Vp_*b* $OH + AsO_4^{3-} + 2H^+ = Vp\_b\,HAsO_4^- + H_2O$	log K_b^2	22.09	25.74	21.60	22.34
		13. Vp_*b* $OH + AsO_4^{3-} + H^+ = Vp\_b\,AsO_4^{2-} + H_2O$	log K_b^3	13.76	15.28	10.41	8.70
		14. Vp_*b* $OH + AsO_4^{3-} = Vp\_b\,OHAsO_4^{3-} + H_2O$	log K_b^4	4.52	8.92	7.69	10.54
	PO_4	15. Vp_*b* $OH + PO_4^{3-} + 3H^+ = Vp\_b\,H_2PO_4 + H_2O$	log K_b^5	26.26	27.53	31.40	32.80
		16. Vp_*b* $OH + PO_4^{3-} + 2H^+ = Vp\_b\,HPO_4^- + H_2O$	log K_b^6	24.00	24.30	24.16	24.89
		17. Vp_*b* $OH + PO_4^{3-} + H^+ = Vp\_b\,PO_4^{2-} + H_2O$	log K_b^7	15.75	17.54	17.31	13.56
		Surface sorption site (moles)	m_b	1.356×10^{-4}	4.761×10^{-5}	2.153×10^{-5}	6.50×10^{-5}
Mn_*c*	Mn^{2+}	18. Mn_*c* $OH + Mn^{2+} = Mn\_c\,OMn^+ + H^+$	log K_{mn}^1	−0.011	−0.002	-9.030×10^{-5}	
		Surface sorption site (moles)	m_{mn}	8.055×10^{-6}	6.574×10^{-6}	8.642×10^{-6}	
		Presorbed concentrations (μmol/kg sediment)	As(V)	4.0	28.3	0.18	
			PO_4	123.4	115.9	194.7	
			Mn	16.9	17.8	110.5	
		Solution complex formation constants					
		19. MOPS−H + Mn^{2+} = MOPS−Mn^+ + H^+	log K_{MOPS}			4.22 (Ref *a*)[a]	
		20. MES−H + Mn^{2+} = MES−Mn^+ + H^+	log K_{MES}			3.59 (Ref *b*)[b]	
		Oxidation rate constant (L/mol/s)	k			1.919×10^{-2}	5.4×10^{-6}
		Half saturation constant (mol/L)	K_s			5.660×10^{-3}	
		Exponential term	α			0.949	

[a] *Anwar and Azab* [1999].
[b] *Azab and Anwar* [2012].

3. Results and Discussion

3.1. Experimental Results

3.1.1. Adsorption Experiments

The concentration-dependent adsorption of As(III) on the Pleistocene sediment produced nonlinear isotherms in both NaCl and artificial groundwater (AGW) solutions (Figure 1). For the highest tested arsenic concentration (25 μmol/L), and in the absence of any competing solutes, the maximum amount of As(III) adsorbed was 0.26 μmol/g of sediment. This amount was reduced to 0.19 μmol/g sediment for the case where an artificial groundwater (AGW) solution containing PO_4 and HCO_3^- was used, suggesting competition for the surface sites. Dissolved As(V) was not detected in any sample. The equilibrium pH of the samples ranged from 6.3 to 6.4 at the end of the adsorption experiment. The maximum As(III) adsorbed on Van Phuc Pleistocene sediment under NaCl conditions was considerably higher than the amount adsorbed on Pleistocene sediments from Bangladesh [*Stollenwerk et al*., 2007] and Holocene sediments from Nam Du, Vietnam [*Thi Hoa Mai et al*., 2014]. However, the maximum As(III) adsorbed on Bangladesh sediments was approximately 20% lower than that for As(V) [*Stollenwerk et al*., 2007] (Figure 1). This, not surprisingly, affirms differing adsorption characteristics for both arsenic species on natural sediments, contrary to that on pure Fe-oxide minerals [*Dixit and Hering*, 2003; *Goldberg*, 2002].

3.1.2. Competition With Phosphate

The results of the phosphate experiments suggested competition between PO_4 and As(III) for the surface sites (Figure 2). The reduction in As(III) adsorption with increasing PO_4 concentrations was least visible in the experiment with low initial As(III) concentrations (1 μmol/L), while becoming more significant when initial As(III) concentrations was 7.5 μmol/L. In the latter experiment, the overall adsorption of As(III) decreased

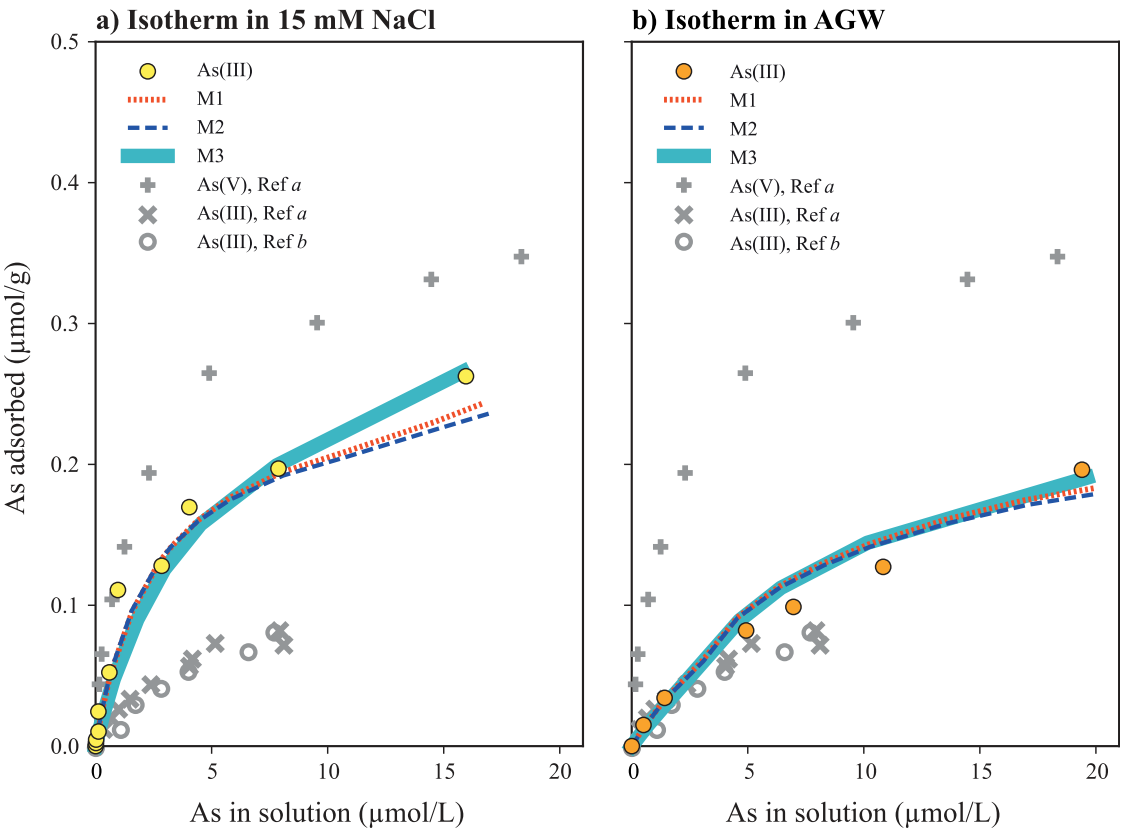

Figure 1. Adsorption Isotherm. Concentration-dependent adsorption of As(III) on Pleistocene sediments in (a) 15 m*M* NaCl and (b) artificial groundwater (AGW) solutions. Both experiments produced nonlinear isotherms with a maximum amount of As(III) adsorbed equaling to 0.26 μmol/g of sediment in NaCl solution. This amount was reduced to 0.19 μmol of As(III) adsorbed per g of sediment in the presence of competing solutes (OH^-, PO_4, and HCO_3) in AGW solution. The amount of adsorbed As(III) in the experiments was determined by difference between initial and final aqueous concentrations. The outputs from three surface complexation model variants M1 (red dotted line), M2 (blue dashed line), and M3 (blue solid line) are plotted here. Models M1 and M2 assume known (i.e., fixed) and unknown (i.e., estimated) amounts of presorbed As(V) on sediments, respectively. In comparison, model M3 includes production of As(V) from oxidation of dissolved As(III) by sediment-bound Mn-oxides. All three models captured the observed trend of isotherm data sets reasonably well. Ref *a*: *Stollenwerk et al*. [2007] and Ref *b*: *Thi Hoa Mai et al*. [2014].

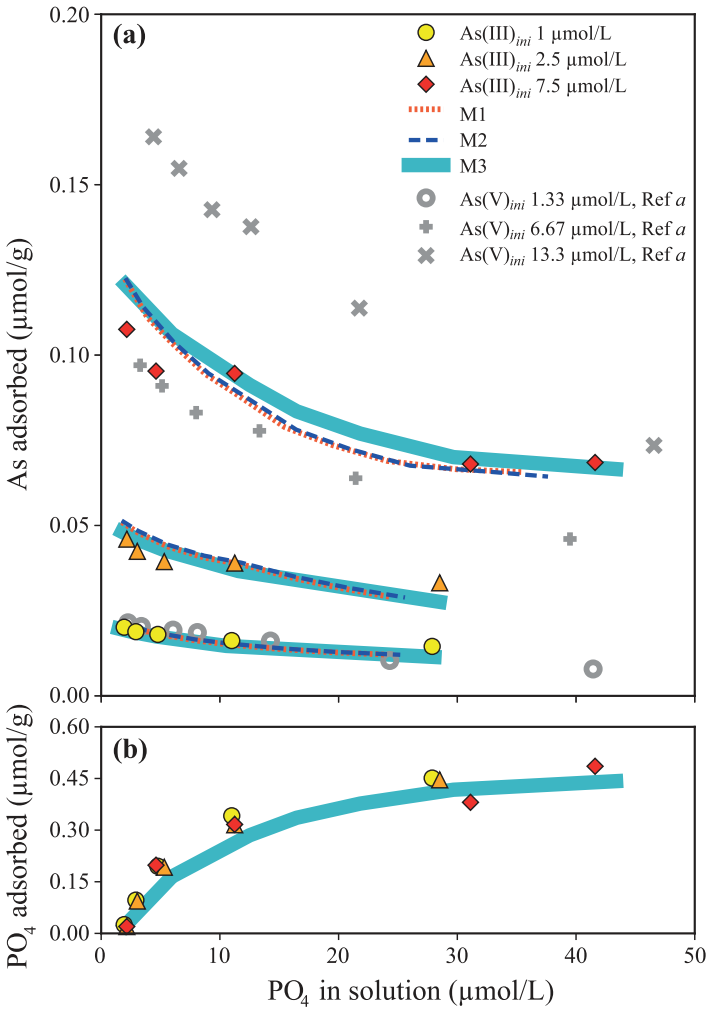

Figure 2. Competitive adsorption of As(III) and PO_4. Adsorption behavior of As(III) on Pleistocene sediments in presence of competing solute PO_4, determined in 15 m*M* NaCl solution at initial As(III) concentrations of 1.0, 2.5, and 7.5 µmol/L and initial PO_4 concentrations of 3, 6, 12, 24, 48, and 60 µmol/L. (a) As(III) adsorption decreased with increasing PO_4 concentrations in all experiments with up to 36% decline in the experiment with highest initial As(III) concentration. (b) On the contrary, increasing As(III) concentrations had no effect on PO_4 adsorption. The amount of adsorbed As(III) in the experiments was determined by difference between initial and final aqueous concentrations. The outputs from three surface complexation model variants M1 (red dotted line), M2 (blue dashed line), and M3 (blue solid line) are plotted here. Models M1 and M2 assume known (i.e., fixed) and unknown (i.e., estimated) amounts of presorbed As(V) on sediments, respectively. In comparison, model M3 includes production of As(V) from oxidation of dissolved As(III) by sediment-bound Mn-oxides. All three models matched the observed data reasonably well. Ref *a*: *Stollenwerk et al.* [2007].

by up to 36% with increasing solution PO_4 concentrations. Similar competition effects have been observed between As(V) and PO_4 [*Kent and Fox*, 2004; *Stollenwerk et al.*, 2007]. On the contrary, increasing solution As(III) concentrations had no effect on the adsorption of PO_4 on the sediment. Dissolved As(V) was not detected in any sample.

3.1.3. Effects of pH

The effect of solution pH on As(III) adsorption behavior was apparent for two investigated initial As(III) concentrations (Figure 3). The data from both experiments suggested an increase in As(III) adsorption by up to 25% with pH increasing from 6 to 8. However in both experiments, the percentage of measured As(III) in the solutions decreased from 90% to 50% with increasing pH while the total arsenic concentration remained relatively constant. Initially, this was assumed to be the redistribution of sorbed As(III) and As(V) species on the sediment surface sites influenced by solution pH, similar to previously observed behavior on Pleistocene sediment [*Stollenwerk et al.*, 2007] and various mineral phases [*Dixit and Hering*, 2003; *Goldberg*, 2002]. However, if all of the presorbed 4.0 µmol of As(V) per kg of Van Phuc sediment sample [*Eiche*, 2009; *Eiche et al.*, 2008] was to be mobilized, it would only be equivalent to 0.16 µmol/L of As(V) in solution, which was well under the maximum As(V) measured (1.47 µmol/L). This implies that there is either some uncertainty in the measurement of presorbed As(V) on sediment surface sites or that As(V) was produced from (partial) oxidation of the As(III) added to the solution.

3.2. Model-Based Analysis of Arsenic Adsorption

The geochemical modeling approach, used here to interpret the data and to establish a more widely usable SCM, included both the surface complexation reactions and any secondary geochemical reactions that may have proceeded during the batch experiments as a result of the experimental procedure. The identification of these secondary reactions and their influence on arsenic adsorption behavior was not clear initially, and the model-based analysis of the experimental data was required to determine their relevance. Modeling was started with what was considered to be the simplest possible set of reactions, before model complexity was increased to account to account for additional processes.

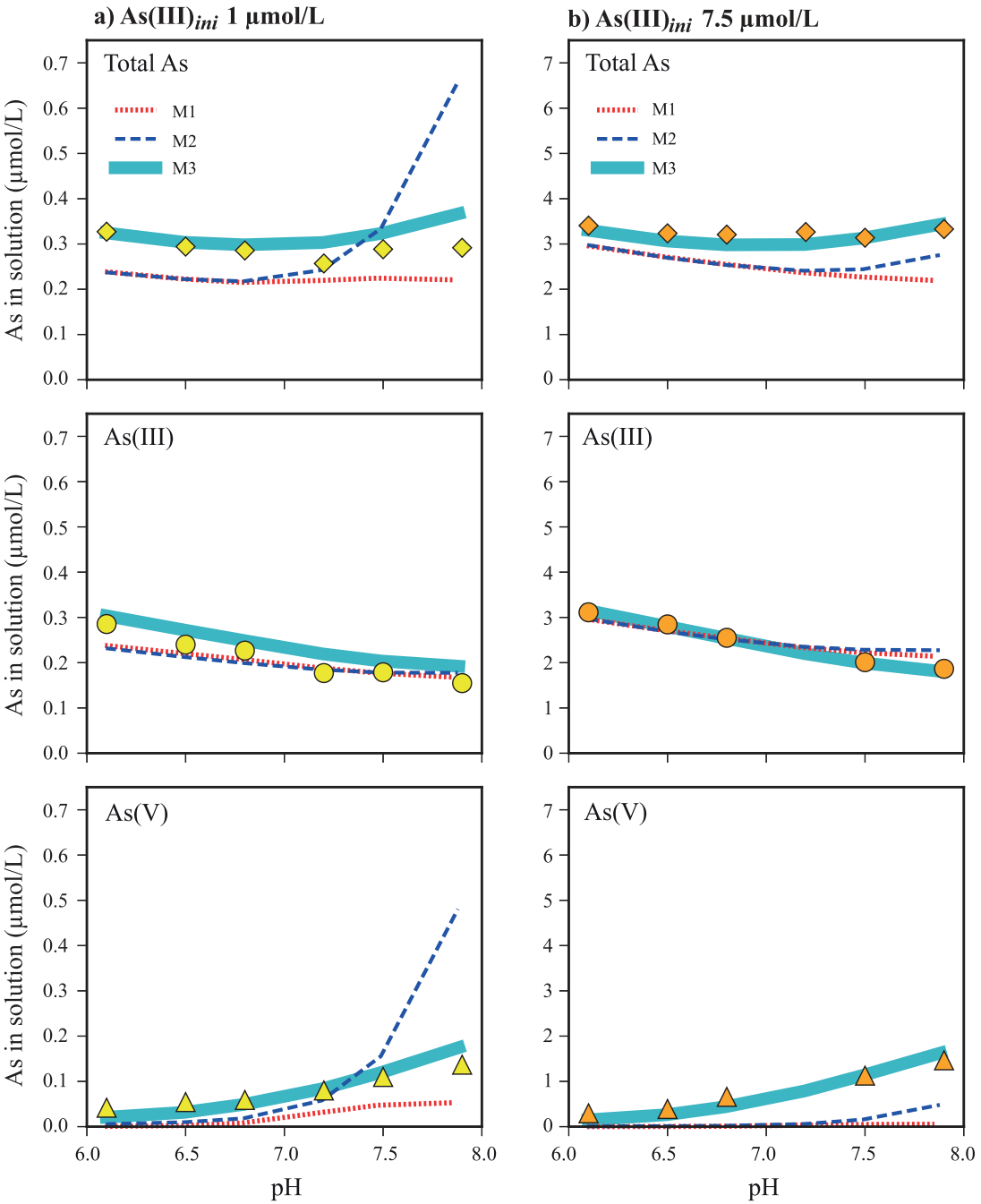

Figure 3. Effects of pH. As(III) sorption behavior on Pleistocene sediments with varying solution pH, determined at initial As(III) concentrations of (a) 1 µmol/L and (b) 7.5 µmol/L in 15 m*M* NaCl solution. The solution pH was modified to 6.1 and 6.5 using MES buffer, and to 6.8, 7.2, 7.5, and 7.9 using MOPS buffer. In both experiments (Figures 3a and 3b), the amount of dissolved total arsenic remained unaffected with increasing solution pH while the concentrations of dissolved As(III) increased by up to 25%. Also, significant amount of As(V) was mobilized with increasing solution pH. The outputs from three surface complexation model variants M1 (red dotted line), M2 (blue dashed line), and M3 (blue solid line) are plotted here. Models M1 and M2 assume known (i.e., fixed) and unknown (i.e., estimated) amounts of presorbed As(V) on sediments, respectively. The concentration of dissolved As(V) could not be explained by models M1 and M2 where desorption of presorbed As(V) was considered from sediment surface sites alone. In model M3, buffers MES and MOPS were allowed to mobilize presorbed Mn(II) from sediment-bound Mn-oxides by forming strong solution complexes between buffers MES/MOPS and Mn^{2+} ions. This process led to an increase in the reactive surface sites on Mn-oxides for As(III) to undergo oxidation into As(V). Model M3 produced the best calibration for the observed experimental data.

3.2.1. Basic Surface Complexation Model (Model M1)

Initial modeling of the experimental results considered only surface complexation reactions, i.e., any secondary geochemical reactions were assumed to play no role. The surface complexation reactions considered in these simulations were based on the model of *Stollenwerk et al.* [2007]. We started with a reaction network that included only one type of mineral-hosted surface site (Vp_*a*). The reaction network included As(III) and PO_4 surface complexation reactions as well as the protonation and deprotonation reactions of the −OH functional group on Vp_*a*. The adopted model was modified based on the hypothesis of *Thi Hoa Mai et al.* [2014] who suggested that the adsorption characteristics of As(III) and As(V) may be different depending on the mineral-hosted surface sites. Consequently, an additional surface site (Vp_*b*) and the corresponding surface complexation reactions of As(V) and PO_4 were included in the model (Tables 1 and 2). As(III) and As(V) were decoupled from the redox equilibrium, usually assumed in the standard PHREEQC database. Initial model simulations included only the surface complexation reactions of As(III), As(V), and PO_4, with the amount of presorbed As(V) on the sediment set to the previously determined value of 4.0 μmol/kg [*Eiche*, 2009; *Eiche et al.*, 2008]. The model was calibrated against the observation data from all experiments using PSO alone. This model (M1) was able to simulate concentration-dependent adsorption of As(III), its competition with PO_4, and the pH effects reasonably well (Figures 1–3). However, model M1 was unable to reproduce the observed aqueous As(V) concentrations in the two pH experiments (Figure 3).

3.2.2. Surface Complexation Reactions With Uncertain Presorbed Concentrations (Model M2)

The observed aqueous As(V) concentrations in the pH experiments could have potentially been desorbed from sediment surface sites during the batch experiments. However, mass balance calculations suggested that the previously determined amount of presorbed As(V) [*Eiche*, 2009; *Eiche et al.*, 2008] could not alone explain these observed aqueous As(V) concentrations. As a result, model M1 was revised to include the concentration of presorbed As(V) as an estimated model parameter and its value was estimated during the model calibration via PSO alone. This revised model, M2, was again able to achieve a good agreement with all measured As(III) data but did not yield significantly improved results for As(V). The modeled As(V) concentrations were overestimated for the experiment that used low initial As(III) concentrations, while modeled concentrations were underestimated for the experiment with high initial As(III) concentrations (Figure 3). From this result, it was concluded that in the pH experiments some redox transformations from As(III) to As(V) must have occurred and the model required further revision.

3.3. Surface Complexation Reactions and Secondary Geochemical Reactions

To identify and quantify the secondary geochemical reactions responsible for the redox transformation from As(III) to As(V), and to understand their influence on arsenic adsorption behavior, concentrations of other solutes in the solution were closely inspected, and additional processes were considered to test variations of the conceptual model. Upon examination, the species that stood out the most was the measured dissolved manganese, i.e., Mn(II) ions.

3.3.1. Release of Mn(II) Ions

Distinctly higher concentrations of Mn(II) ions, or Mn^{2+}, were observed in the pH experiments (max 4.19 μmol/L) compared to those obtained from the isotherm and phosphate experiments (max 0.56 μmol/L) (Figure 4). The blank samples from all experiments contained Mn^{2+} concentrations below the detection limit of 0.02 μmol/L. The most likely sources of Mn^{2+} were thought to be either (i) manganese-bearing minerals or (ii) presorbed Mn(II) on sediment surface sites.

Dissolution and release of Mn^{2+} could involve either reduced manganese minerals such as rhodochrosite ($Mn^{II}CO_3$) or the reduction of Mn-oxides, which would only proceed in the presence of a suitable electron donor. Under the prevailing experimental conditions, As(III) was the only potential electron donor. However, the As(III) concentration of 1.0 μmol/L in one of the pH experiments was too low to explain the observed magnitude of Mn^{2+} released through direct reduction of Mn-oxides. Furthermore, the dissolution of rhodochrosite would be primarily controlled by the ion activity product of Mn^{2+} and CO_3^{2-}, which is not consistent with the fact that enhanced Mn^{2+} release occurred only in the pH experiments (range 6–7) and not in other experiments (pH range 6.3–6.6). Similarly, the observed phenomena is not easily explained by desorption since a fixed amount of presorbed Mn(II) cannot produce higher concentrations of Mn^{2+} in the pH experiments alone (Figure 4). The decreasing concentrations of Mn^{2+} with increasing pH or PO_4 concentrations could be attributed to higher sorption of cations surface sorption sites saturated with OH or PO_4

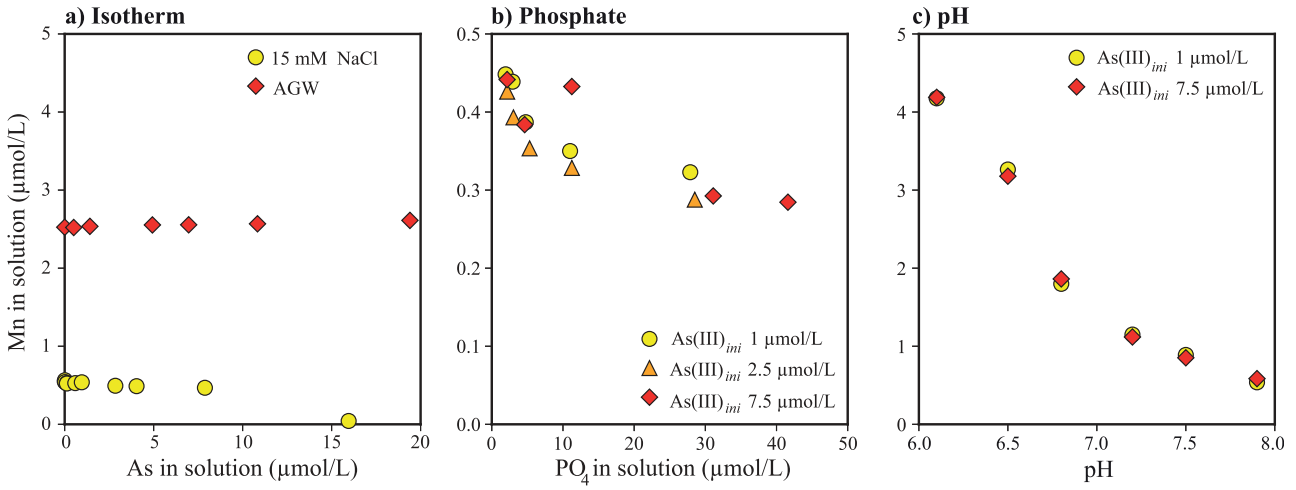

Figure 4. Aqueous Mn(II) concentrations. The concentrations of aqueous Mn(II) are plotted for experiments in which As(III) sorption behavior on Pleistocene sediments was determined for varying (a) As(III) concentrations, in 15 m*M* NaCl and artificial groundwater (AGW) solutions; (b) PO_4 concentrations; and (c) solution pH values. Exceptionally high amounts of Mn(II) concentrations were measured in pH experiments compared to other experiments. This observation was attributed to the mobilization of presorbed Mn(II) from sediment-bound Mn-oxides due to the formation of strong solution complexes between buffers MES/MOPS and Mn^{2+} ions.

anions. Therefore, some geochemical process, producing relatively high Mn^{2+} concentrations, must have been occurring in the pH experiments that was were not occurring in the remaining experiments.

The main difference between the pH experiments and the other experiments was that organic buffers, MOPS and MES, were employed to maintain pH in addition to the background NaCl solution. While these buffers are generally considered not to undergo any metal complex formation for the investigated pH range, Anwar and Azab [*Anwar and Azab*, 1999; *Azab and Anwar*, 2012] suggested that Mn^{2+} complexes can be formed. They also determined complex formation constants for MES and MOPS with Mn^{2+}:

$$\mathrm{MOPS{-}H{+}Mn^{2+}{=}MOPS{-}Mn^{+}{+}H^{+}} \quad \log K_{\mathrm{MOPS}} = 3.54 \tag{19}$$

$$\mathrm{MES{-}H{+}Mn^{2+}{=}MES{-}Mn^{+}{+}H^{+}} \quad \log K_{\mathrm{MES}} = 3.48 \tag{20}$$

Therefore, these buffers have the potential to enhance Mn(II) desorption from the sediment surface sites. This process can indirectly promote significant As(III) oxidation by Mn-oxides. In order to see this, first a brief review of As(III) oxidation by Mn-oxides is provided in the following.

3.3.2. As(III) Oxidation by Manganese Oxides

The oxidation of As(III) by both laboratory synthesized and naturally occurring manganese oxides has been extensively discussed in the literature through experimental and geochemical modeling studies [*Amirbahman et al*., 2006; *Bai et al*., 2016; *Nesbitt et al*., 1998; *Scott and Morgan*, 1995; *Stollenwerk et al*., 2007; *Tournassat et al*., 2002; *Ying et al*., 2011]. These studies consider the following overall reaction for As(III) oxidation by Mn-oxides:

$$\mathrm{MnO_2 + H_3As^{III}O_3 + 2H^+ \rightarrow Mn^{2+} + H_3As^{V}O_4 + H_2O} \tag{21}$$

The details of the mechanisms proposed for the oxidation of As(III) by Mn-oxides vary in the literature and usually involve a series of steps. However, there is a general agreement that the adsorption of As(III) onto Mn-oxide surface sites is the initiating step for the oxidation reaction [*Amirbahman et al*., 2006]. Subsequently, adsorbed As(III) undergoes kinetically controlled oxidation and releases As(V) into the solution [*Nesbitt et al*., 1998]. In order to model this, there must be a mechanism for initiating the oxidation of As(III) only after it has sorbed onto Mn-oxides contained within the sediment.

The rate of As(III) oxidation by Mn-oxides could be affected by solution pH. A recent experimental study [*Wu et al*., 2015] showed that the oxidation rate was higher at solution pH 6 compared to that at pH 3. However, to the best of our knowledge, there are no experimental studies that have rigorously investigated the effects of pH, above 6, on the rate of As(III) oxidation. In this study, we explicitly consider the effects of pH and therefore must have a mechanism for quantifying these effects in our model.

3.3.3. Revised Conceptual Model (Model M3)

The addition of organic buffers in the pH experiments could promote significant As(III) oxidation by Mn-oxides. With the addition of an organic buffer, presorbed Mn(II) is mobilized due to formation of stronger solution complexes:

$$\text{Mn\_}c\text{OMn}^{+} + \text{Orgb}-\text{H} \rightarrow \text{Mn\_}c\text{OH} + \text{Orgb}-\text{Mn}^{+} \tag{22}$$

where Mn_*c* denotes a surface site on Mn-oxide and Orgb is either MOPS or MES. The relative increase in the number of surface sites occupied by OH species (Mn_*c*OH) allows for an increased amount of dissolved As(III) to adsorb and undergo kinetically controlled oxidation.

These processes are incorporated into model M2 by simulating the apparent secondary geochemical reactions as follows: (i) the formation of Mn^{2+} complexes with organic buffers (MOPS and MES) and (ii) the oxidation of As(III) by Mn-oxide. The revised reaction network included an additional surface site (Mn_*c*), assumed to be associated with Mn-oxides and was occupied mostly by Mn(II) species prior to the start of the adsorption experiment. Once the organic buffer displaces Mn(II) and results in increased Mn_*c*OH sites, As(III) oxidation proceeds using a rate law modified from the literature [*Tournassat et al*., 2002; *Ying et al*., 2011] as

$$\frac{d[\text{As(III)}]}{dt} = k \times \left(\frac{[\text{As(III)}]}{K_s + [\text{As(III)}]}\right) \times \{\text{OH}^{-}\}^{\alpha} \times \frac{([\text{Mn\_}c\text{OH}] - [\text{Mn\_}c\text{OMn}^{+}])}{\text{Total}[\text{Mn\_}c]} \tag{23}$$

where k is a rate constant (L/mol/s), $[\text{As(III)}]$ is the total amount of all As(III) solution species (mol/L), K_s is a half-saturation constant for As(III) (mol/L), $\{\text{OH}^{-}\}$ is the activity of OH^{-} ions (mol/L), α is an exponential term, $[\text{Mn\_}c\text{OH}]$ represents the moles of surface sites (Mn_*c*OH) per litre of solution, $[\text{Mn\_}c\text{OMn}^{+}]$ represents the moles of Mn(II)-occupied surface sites ($\text{Mn\_}c\text{OMn}^{+}$) per liter of solution and $\text{Total}[\text{Mn\_}c]$ represents the total moles of surface sites on Mn-oxides. These processes, combined with model M2, resulted in a more complex model denoted as M3 (Figure 5).

In model M3, the oxidation rate was allowed to proceed kinetically over a period of 7 days, corresponding to the period between the start of the batch experiment and sample collection. The exponential term (α) was included for the activity of OH^{-} ions to establish a relationship between solution pH and the oxidation rate, and its value was estimated during model calibration via PSO, followed by a local calibration step via PEST with Tikhonov regularization. As shown in Figures 1–3, model M3 was capable of explaining all measured concentrations of As(III), As(V), total arsenic and PO_4. The formation of the solution complexes between the organic buffer and Mn^{2+}, and its effects on dissolved As(V) concentrations in the pH experiments, can be demonstrated with model M3 by (de)activating reaction (22) (a comparison of model outputs is shown in the supporting information Figure S2). The process-based geochemical modeling framework in model M3 identifies and incorporates secondary geochemical reactions (As(III) oxidation) and observed data (Mn^{2+} concentrations) to derive an improved interpretation of experimental data.

The sensitivity of each calibrated parameter in model M3 was calculated using the PEST software in order to measure each parameter's influence on the observations, which consist of different data types (As(III), total arsenic, PO_4, and Mn^{2+}). It is important to note here that since the model is nonlinear, these sensitivities are only accurate for the calibrated parameter values and may be different for different parameter values. The apparent equilibrium constant log K_a^2 for reaction (4) in Table 3 was identified as the most sensitive parameter for all observations due to the complex interactions and competition of other species with As(III). The parameter log K_a^5 (reaction (7), Table 3) was also identified as a very sensitive parameter as it represents the sorption of $H_2PO_4^{-}$ species which is dominant over the pH range considered in the PO_4 experiments. In contrast, the parameters log K_b^1 (reaction (11), Table 3) and log K_b^2 (reaction (12), Table 3) were the least sensitive parameters, possibly due to the low concentrations of As(V) that were present in the experiments. The parameters log K_a^2 and log K_a^5 were strongly correlated, which demonstrates a strong competition between As(III) and PO_4 for sorption on site Vp_*a*. This correlation was remediated with the help of Tikhonov Regularization by matching the parameter values to the prior information obtained from *Stollenwerk et al*. [2007]. Some of the effects of correlation amongst parameter estimates may still persist even with regularization, e.g., for parameters that do not have prior information in the literature such as pK_a^2 (reaction (2), Table 3) and log K_a^2. However, these effects would likely be small as half of the parameters considered in this study have prior information taken from the literature. Furthermore, quantitatively addressing the effects of parameter uncertainty is beyond the scope of this study.

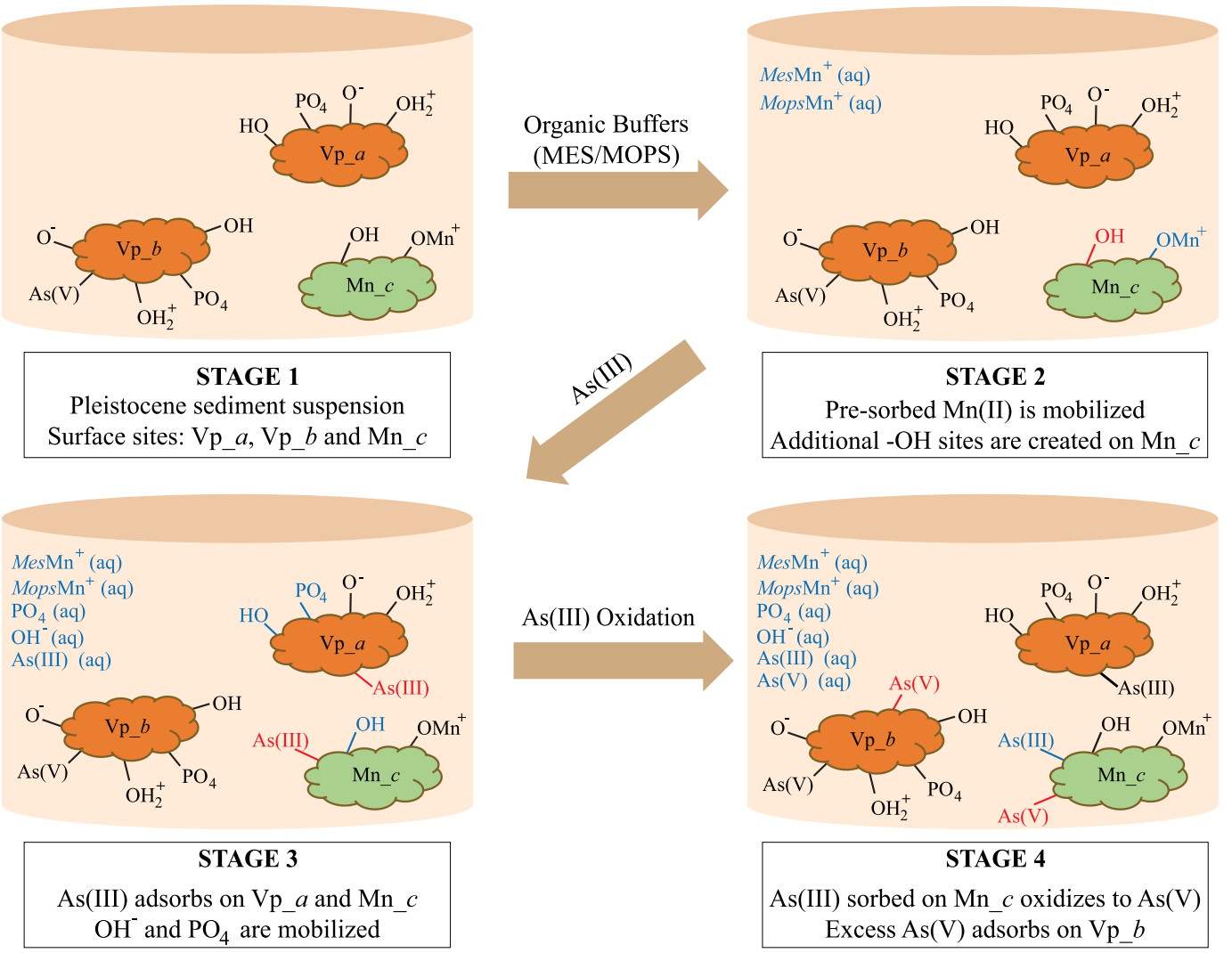

Figure 5. Model M3 conceptualization. The surface complexation model M3 includes three types of surface sites on Pleistocene sediments. Site Vp_*a* complexes with As(III), PO_4, and –OH; site Vp_*b* with As(V), PO_4, and –OH; and site Mn_*c* complexes with –OH, Mn(II), and As(III) species. The presorbed amount of As(V) on sediments was considered unknown and was, therefore, estimated during model calibration. Addition of buffers MES and MOPS allowed for mobilization of presorbed Mn(II) from sediment-bound Mn-oxides by forming strong solution complexes. This process increases the number of Mn_*c* sites available for As(III) to undergo oxidation into As(V). Model M3 produced the best calibration for the observed data in all experiments.

The competition effect between As(III) and PO_4 as postulated in model M3 is better illustrated in Figure 6. In the isotherm experiments, increasing As(III) solution concentrations result in mobilization of PO_4 either presorbed on sorption sites or added to the solution. In the phosphate experiments, increasing PO_4 competes for the surface sites with the fixed amount of As(III) added to the solutions. In the pH experiments, variations in the adsorption of As(III) and As(V) appear to be negligible over the experimental pH range.

3.4. Implications for Field-Scale Arsenic Transport and Retardation

The simulation of As(III) oxidation by Mn-oxides was considered in our model through a somewhat simplistic approach based on the widely accepted overall reaction (21). Additional data, outside the scope of this study, would be required in order to tightly constrain a more refined model of the various mechanisms that were previously hypothesized in some studies that specifically investigated the role of Mn-oxides on As(III) oxidation [*Amirbahman et al.*, 2006; *Tournassat et al.*, 2002]. However, the occurrence of Mn(II) mobilization by organic buffers points to a very important scenario that could affect arsenic mobility at field sites. Migrating groundwater from shallow Holocene aquifers into Pleistocene aquifers contains large amount of dissolved organic carbon (DOC) [*Harvey et al.*, 2002]. The DOC is composed of various organic ligands

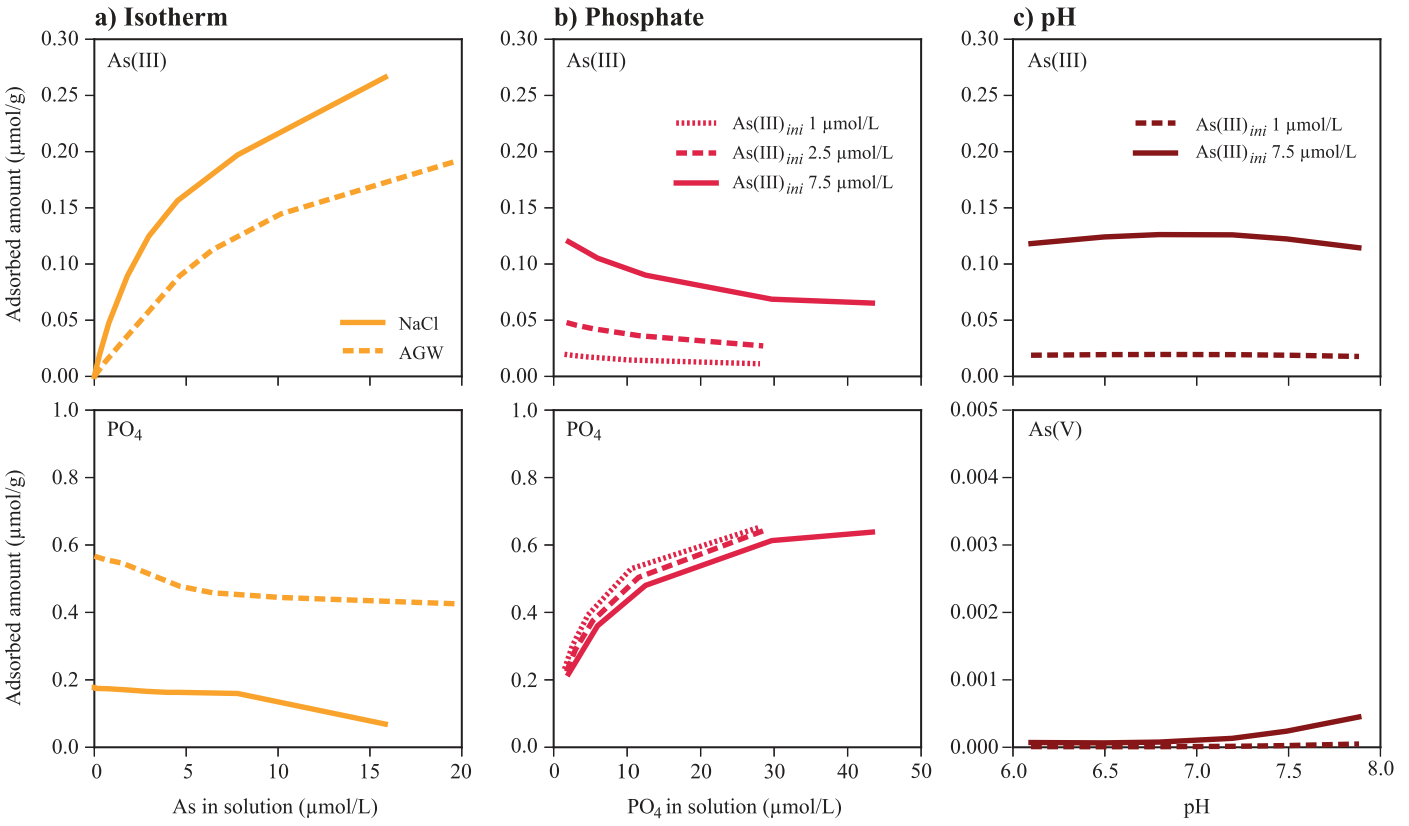

Figure 6. Adsorbed concentrations in model M3. The amount of adsorbed As(III), As(V), and PO_4 per g of sediment calculated in model M3 are plotted for As(III) sorption experiments on Pleistocene sediments under varying (a) As(III) concentrations, in 15 m*M* NaCl and artificial groundwater (AGW) solutions; (b) PO_4 concentrations; and (c) solution pH values. The competition between As(III) and PO_4 is clear in the model results for experiments (Figures 6a and 6b). In the former, increasing amount of adsorbed As(III) is responsible for mobilizing presorbed PO_4 while in the latter, As(III) adsorption is strongly affected by the increasing amount of solution PO_4. In contrast, (Figure 6c) pH effect on adsorbed As(III) and As(V) was negligible.

including organic acids, amino acids, sugars, phenols, and other compounds which are known to form solution complexes with divalent ions, such as Mn^{2+} [*Gillispie et al*., 2016; *Norvell*, 1988], sorbed on Mn-oxide minerals naturally present in the Pleistocene sediments [*Eiche et al*., 2008]. This could further result in the oxidation of dissolved As(III), as observed in our pH experiments. As(V) produced from redox transformations could sorb on the additional sites present on the sediments or precipitate with aqueous Mn(II). Reducing groundwater from Holocene aquifers also contains high concentrations of dissolved Fe(II) which, is preferentially oxidized to Fe(III)-(hydro)oxides by Mn-oxides in comparison to As(III) [*Wu et al*., 2015]. These newly formed Fe-minerals have a high affinity for both As(III) and As(V) adsorption and greatly improve arsenic attenuation in groundwater [*Pierce and Moore*, 1982; *Smith et al*., 2017].

We expect that the relevance of the above discussed geochemical processes will vary from site to site and as such a more generic prediction of their impact is beyond the scope of this study. However, we demonstrate the consideration of the primary surface complexation reactions from model M3 within a highly idealized 1-D reactive transport model developed with PHT3D [*Prommer et al*., 2003] that is loosely based on a 2.5 km long transect at the Van Phuc site [*van Geen et al*., 2013]. The main purpose of these simulations is to illustrate the impact of varying geochemical conditions and assumptions on arsenic migration rates. In the simulations, we used the surface complexation reactions of As(III), As(V), and PO_4 as defined for model M3. A range of different fractions of sorption site densities calculated for Pleistocene sediments in model M3 were employed along with varying compositions of Holocene groundwater. Figure 7 illustrates the sensitivity of simulated arsenic concentration profiles to varying geochemical conditions and parameters after a 50 year long intrusion of Holocene groundwater into a Pleistocene aquifer. The results illustrate the strong impact of the magnitude of the aqueous arsenic concentrations as well as a significant impact of the aqueous phosphate concentrations on arsenic migration rates within the Pleistocene aquifer. Figure 7 further

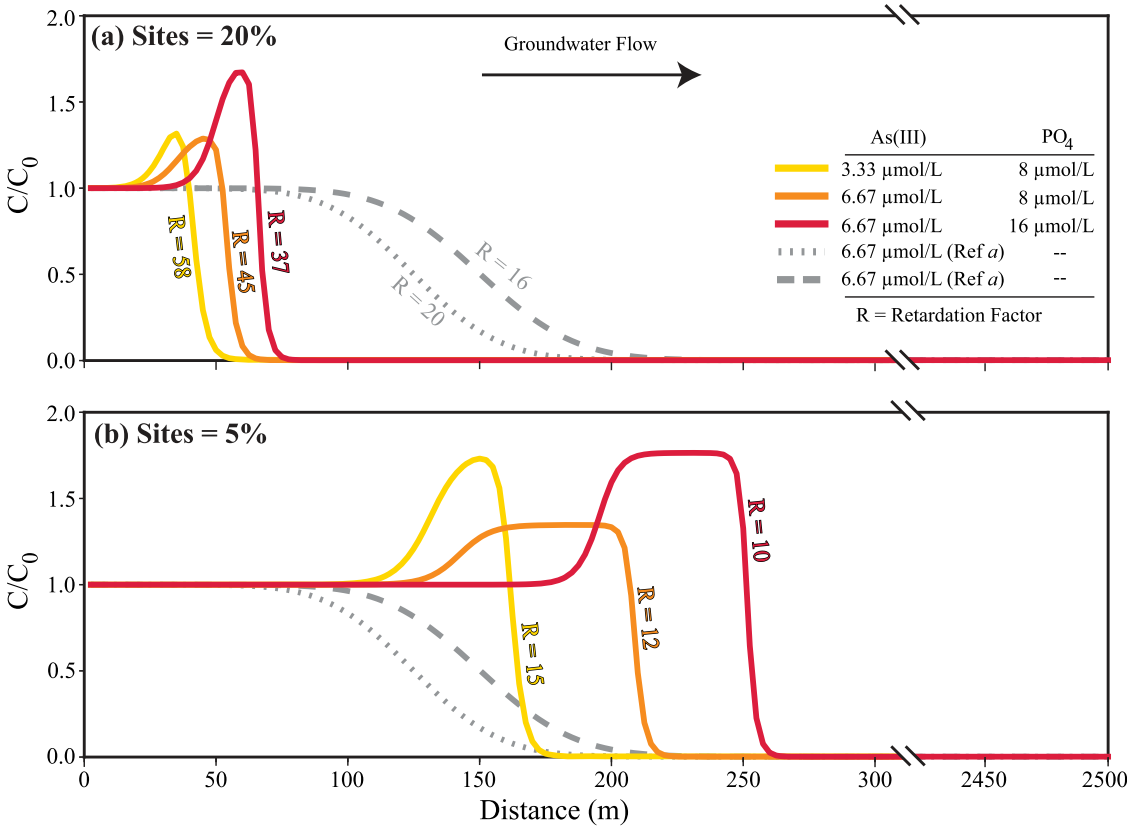

Figure 7. 1-D reactive transport simulations. An idealized one-dimensional (1-D) model was developed that considers the intrusion of high-arsenic Holocene groundwater into a low-arsenic Pleistocene aquifer over 50 years to a distance of 2.5 km. The arsenic concentration profiles produced using this model are illustrated for sediment surface sites equal to (a) 20% and (b) 5% of laboratory sediments under varying As(III) and PO_4 concentrations of incoming Holocene groundwater. The physical accessibility of the sediment sorption sites at field-scale is shown to have a significant impact on the simulated arsenic retardation factor. Ref *a*: *van Geen et al*. [2013].

shows the significant impact of the sediment sorption sites that would be physically accessible at field-scale and the corresponding variation in the effective retardation factor values for arsenic (R_{min} = 10 for 5% of sites accessible; R_{max} = 58 for 20% of sites accessible). This result reasserts that the inaccessibility of sorption sites and hydrogeological heterogeneity could produce lower arsenic retardation when upscaling laboratory models to field-scale [*Radloff et al*., 2011]. The almost vertical shape of the arsenic fronts is controlled by strong adsorption characteristics determined in our experiments as compared to the more dispersed plume fronts produced by linear sorption models [*van Geen et al*., 2013]. The simulated concentration peaks near the plume fronts are due to the competition between As(III) and PO_4 for adsorption on the sediment surface sites.

4. Conclusions

In this study, we performed a quantitative characterization of As(III) adsorption behavior onto natural Pleistocene sediments, through anoxic batch experiments under a range of field-relevant geochemical conditions and inverse geochemical modeling. Based on the results, As(III) adsorption onto sediment surface sites was found to be nonlinear, similar to the previous study of *Stollenwerk et al*. [2007]. The observed sorption characteristics found dissolved inorganic phosphate (PO_4) competes with As(III) for the sorption sites and the solution pH in the investigated range between 6 and 8 had a negligible effect on total arsenic sorption. Contrary to the previously reported study by *Stollenwerk et al*. [2007], the possibility of As(III) oxidation by naturally abundant Mn-oxides was examined in all of our experiments and was only observed in the pH experiments.

A series of models was developed for this study with varying complexity in order to identify the processes governing As(III) sorption and oxidation. Upon rigorous calibration of each model, it became apparent that

an additional process was required in order to simulate the As(III) oxidation in the pH experiments. The primary difference between the pH experiments and the remaining experiments was the addition of organic buffers, MOPS and MES. In the model simulations, these buffers were shown to be sensitive to As(III) oxidation by displacing Mn(II) from the sediment surfaces. The desorption of Mn(II) from Mn-oxide surface sites driven by formation of aqueous complexes with organic buffers and the subsequent oxidation of As(III) by Mn-oxides were found to be necessary processes in order to most accurately reproduce observed experimental concentrations in the pH experiments.

For the model developed in this study, As(III) sorption behavior was simulated through three types of sorption sites. One type of site allowed for competitive sorption between As(III) and PO_4, while the second site represented sedimentary Mn-oxides that were presorbed with divalent metal ions, such as Mn(II). We hypothesized that dissolved organic matter in natural waters could exert an influence that is analogous to that of the organic buffers used in our pH experiments and affect the partitioning of presorbed metal ions by forming solution complexes with them. This could result in free Mn-oxide sorption sites which promote oxidation of As(III) to arsenate, As(V). This required a third type of site in the model that allowed for competitive sorption between As(V) and PO_4. Our study illustrates how a process-based inverse geochemical modeling framework can identify and incorporate secondary geochemical reactions (e.g., kinetically controlled As(III) oxidation) and observed data (Mn^{2+} concentrations) to derive an improved interpretation of laboratory sorption experiments. The derived model M3 will provide an important basis for future, more detailed and site-specific reactive transport modeling study within Pleistocene aquifers.

Acknowledgments
The authors warmly thank Caroline Stengel, Andreas Voegelin, Anna-Caterina Senn, and Thomas Rüttimann for providing assistance in the laboratory at Eawag. They also thank Elisabeth Eiche for providing the sediment material and Michael Donn and Ilka Wallis for valuable feedback on the manuscript. They acknowledge the financial support provided by UWA, Eawag, and CSIRO through postgraduate scholarship and travel funding. Additional information and data can be found in the supporting information and/or by contacting the corresponding author. The authors declare no competing financial interest.

References

Abdelaziz, R., and M. Zambrano-Bigiarini (2014), Particle Swarm Optimization for inverse modeling of solute transport in fractured gneiss aquifer, *J. Contam. Hydrol.*, *164*, 285–298.

Amirbahman, A., D. B. Kent, G. P. Curtis, and J. A. Davis (2006), Kinetics of sorption and abiotic oxidation of arsenic(III) by aquifer materials, *Geochim. Cosmochim. Acta*, *70*(3), 533–547.

Anwar, Z. M., and H. A. Azab (1999), Ternary complexes in solution. Comparison of the coordination tendency of some biologically important zwitterionic buffers toward the binary complexes of some transition metal ions and some amino acids, *J. Chem. Eng. Data*, *44*(6), 1151–1157.

Azab, H. A., and Z. M. Anwar (2012), Coordination tendency of some biologically important zwitterionic buffers toward metal ion nucleotide complexes at different temperatures, *J. Chem. Eng. Data*, *57*(10), 2890–2895.

Bai, Y., T. Yang, J. Liang, and J. Qu (2016), The role of biogenic Fe-Mn oxides formed in situ for arsenic oxidation and adsorption in aquatic ecosystems, *Water Res.*, *98*, 119–127.

Berg, M., P. T. K. Trang, C. Stengel, J. Buschmann, P. H. Viet, N. Van Dan, W. Giger, and D. Stüben (2008), Hydrological and sedimentary controls leading to arsenic contamination of groundwater in the Hanoi area, Vietnam: The impact of iron-arsenic ratios, peat, river bank deposits, and excessive groundwater abstraction, *Chem. Geol.*, *249*(1–2), 91–112.

Biswas, A., J. P. Gustafsson, H. Neidhardt, D. Halder, A. K. Kundu, D. Chatterjee, Z. Berner, and P. Bhattacharya (2014), Role of competing ions in the mobilization of arsenic in groundwater of Bengal Basin: Insight from surface complexation modeling, *Water Res.*, *55*, 30–39.

Burgess, W. G., M. A. Hoque, H. A. Michael, C. I. Voss, G. N. Breit, and K. M. Ahmed (2010), Vulnerability of deep groundwater in the Bengal Aquifer System to contamination by arsenic, *Nat. Geosci.*, *3*(2), 83–87.

Coello, C. A. C., G. T. Pulido, and M. S. Lechuga (2004), Handling multiple objectives with particle swarm optimization, *IEEE Trans. Evol. Comput.*, *8*(3), 256–279.

Davis, J. A., and D. B. Kent (1990), Surface complexation modeling in aqueous geochemistry, in *Mineral-Water Interface Geochemistry*, edited by M. F. Hochella and A. F. White, pp. 177–260, Miner. Soc. Am., Washington, D. C.

Davis, J. A., J. A. Coston, D. B. Kent, and C. C. Fuller (1998), Application of the surface complexation concept to complex mineral assemblages, *Environ. Sci. Technol.*, *32*(19), 2820–2828.

Dixit, S., and J. G. Hering (2003), Comparison of arsenic (V) and arsenic (III) sorption onto iron oxide minerals: Implications for arsenic mobility, *Environ. Sci. Technol.*, *37*(18), 4182–4189.

Doherty, J. E. (2010), *PEST: Model-Independent Parameter Estimation*, Watermark Numer. Comput., Brisbane, Australia. [Available at www.pesthomepage.org.]

Dzombak, D. A., and F. M. M. Morel (1990), *Surface Complexation Modeling-Hydrous Ferric Oxide*, 416 pp., John Wiley, New York.

Eberhart, R., and J. Kennedy (1995), A new optimizer using particle swarm theory, paper presented at the Sixth International Symposium on Micro Machine and Human Science, 1995. MHS '95, 4–6 Oct 1995, Inst. of Elect. and Electron. Eng., Piscataway, N. J.

Eiche, E. (2009), *Arsenic Mobilization Processes in the Red River Delta, Vietnam—Towards a Better Understanding of the Patchy Distribution of Dissolved Arsenic in Alluvial Deposits*, Karlsruher Inst. of Technol., Karlsruhe, Germany.

Eiche, E., T. Neumann, M. Berg, B. Weinman, A. van Geen, S. Norra, Z. Berner, P. T. K. Trang, P. H. Viet, and D. Stüben (2008), Geochemical processes underlying a sharp contrast in groundwater arsenic concentrations in a village on the Red River delta, Vietnam, *Appl. Geochem.*, *23*(11), 3143–3154.

Eiche, E., U. Kramar, M. Berg, Z. Berner, S. Norra, and T. Neumann (2010), Geochemical changes in individual sediment grains during sequential arsenic extractions, *Water Res.*, *44*(19), 5545–5555.

Fendorf, S., H. A. Michael, and A. van Geen (2010), Spatial and temporal variations of groundwater arsenic in south and southeast Asia, *Science*, *328*(5982), 1123–1127.

Gillispie, E. C., E. Andujar, and M. L. Polizzotto (2016), Chemical controls on abiotic and biotic release of geogenic arsenic from Pleistocene aquifer sediments to groundwater, *Environ. Sci. Processes Impacts*, *18*(8), 1090–1103.

Goldberg, S. (1991), Sensitivity of surface complexation modeling to the surface site density parameter, *J. Colloid Interface Sci.*, *145*(1), 1–9.

Goldberg, S. (2002), Competitive adsorption of arsenate and arsenite on oxides and clay minerals, *Soil Sci. Soc. Am. J.*, *66*(2), 413–421.
Harvey, C. F., et al. (2002), Arsenic mobility and groundwater extraction in Bangladesh, *Science*, *298*(5598), 1602–1606.
Herberlin, A. L., and J. C. Westall (1999), FITEQL: A computer program for the determination of chemical equilibrium constants from experimental data, Version 4.0, *Rep. 99–01*, Chem. Dep., Oreg. State Univ., Corvallis.
Jessen, S., D. Postma, F. Larsen, P. Q. Nhan, L. Q. Hoa, T. K. T. Pham, T. V. Long, P. H. Viet, and R. Jakobsen (2012), Surface complexation modeling of groundwater arsenic mobility: Results of a forced gradient experiment in a Red River flood plain aquifer, Vietnam, *Geochim. Cosmochim. Acta*, *98*, 186–201.
Jung, H. B., M. A. Charette, and Y. Zheng (2009), Field, laboratory, and modeling study of reactive transport of groundwater arsenic in a coastal aquifer, *Environ. Sci. Technol.*, *43*(14), 5333–5338.
Karamalidis, A. K., and D. A. Dzombak (2010), *Surface Complexation Modeling: Gibbsite*, John Wiley, Hoboken, N. J.
Kennedy, J. F., R. C. Eberhart, and Y. Shi (2001), *Swarm Intelligence*, Morgan Kaufmann, San Francisco, Calif.
Kent, D. B., and P. M. Fox (2004), The influence of groundwater chemistry on arsenic concentrations and speciation in a quartz sand and gravel aquifera, *Geochem. Trans.*, *5*(1), 1.
Lowers, H. A., G. N. Breit, A. L. Foster, J. Whitney, J. Yount, M. N. Uddin, and A. A. Muneem (2007), Arsenic incorporation into authigenic pyrite, Bengal Basin sediment, Bangladesh, *Geochim. Cosmochim. Acta*, *71*(11), 2699–2717.
McArthur, J., P. Ravenscroft, D. Banerjee, J. Milsom, K. Hudson-Edwards, S. Sengupta, C. Bristow, A. Sarkar, S. Tonkin, and R. Purohit (2008), How paleosols influence groundwater flow and arsenic pollution: A model from the Bengal Basin and its worldwide implication, *Water Resour. Res.*, *44*, W11411, doi:10.1029/2007WR006552.
Meng, X., and W. Wang (1998), Speciation of arsenic by disposable cartridges, paper presented at the Third International Conference on Arsenic Exposure and Health Effects, The Soc. of Environ. Geochem. and Health, San Diego, Calif.
Michael, H. A., and C. I. Voss (2008), Evaluation of the sustainability of deep groundwater as an arsenic-safe resource in the Bengal Basin, *Proc. Natl. Acad. Sci. U. S. A.*, *105*(25), 8531–8536.
Nesbitt, H. W., G. W. Canning, and G. M. Bancroft (1998), XPS study of reductive dissolution of 7Å-birnessite by H3AsO3, with constraints on reaction mechanism, *Geochim. Cosmochim. Acta*, *62*(12), 2097–2110.
Norvell, W. A. (1988), Inorganic reactions of manganese in soils, in *Manganese in Soils and Plants: Proceedings of the International Symposium on 'Manganese in Soils and Plants'*, edited by R. D. Graham, R. J. Hannam, and N. C. Uren, pp. 37–58, Springer, Dordrecht, Netherlands.
Parkhurst, D. L., and C. A. J. Appelo (1999), *User's Guide to PHREEQC (Version 2) a Computer Program for Speciation, Batch-Reaction, One-Dimensional Transport, and Inverse Geochemical Calculations*, 312 pp., U.S. Geol. Sur. Earth Sci. Inf. Cent., Denver, Colo.
Pierce, M. L., and C. B. Moore (1982), Adsorption of arsenite and arsenate on amorphous iron hydroxide, *Water Res.*, *16*(7), 1247–1253.
Planer-Friedrich, B., J. London, R. B. McCleskey, D. K. Nordstrom, and D. Wallschläger (2007), Thioarsenates in geothermal waters of Yellowstone National Park: Determination, preservation, and geochemical importance, *Environ. Sci. Technol.*, *41*(15), 5245–5251.
Poeter, E. P., and M. C. Hill (1999), UCODE, a computer code for universal inverse modeling, *Comput. Geosci.*, *25*(4), 457–462.
Prommer, H., D. A. Barry, and C. Zheng (2003), MODFLOW/MT3DMS-based reactive multicomponent transport modeling, *Ground Water*, *41*(2), 247–257.
Radloff, K. A., et al. (2011), Arsenic migration to deep groundwater in Bangladesh influenced by adsorption and water demand, *Nat. Geosci.*, *4*(11), 793–798.
Rawson, J., H. Prommer, A. Siade, J. Carr, M. Berg, J. A. Davis, and S. Fendorf (2016), Numerical modeling of arsenic mobility during reductive iron-mineral transformations, *Environ. Sci. Technol.*, *50*(5), 2459–2467.
Robinson, C., M. V. Brömssen, P. Bhattacharya, S. Häller, A. Bivén, M. Hossain, G. Jacks, K. M. Ahmed, M. A. Hasan, and R. Thunvik (2011), Dynamics of arsenic adsorption in the targeted arsenic-safe aquifers in Matlab, south-eastern Bangladesh: Insight from experimental studies, *Appl. Geochem.*, *26*(4), 624–635.
Scott, M. J., and J. J. Morgan (1995), Reactions at oxide surfaces. 1. Oxidation of As(III) by synthetic birnessite, *Environ. Sci. Technol.*, *29*(8), 1898–1905.
Smedley, P., and D. Kinniburgh (2002), A review of the source, behaviour and distribution of arsenic in natural waters, *Appl. Geochem.*, *17*(5), 517–568.
Smith, R. L., D. B. Kent, D. A. Repert, and J. K. Böhlke (2017), Anoxic nitrate reduction coupled with iron oxidation and attenuation of dissolved arsenic and phosphate in a sand and gravel aquifer, *Geochim. Cosmochim. Acta*, *196*, 102–120.
Stachowicz, M., Hiemstra, T., and van Riemsdijk, W. H. (2008), Multi-competitive interaction of As(III) and As(V) oxyanions with Ca^{2+}, Mg^{2+}, PO_3^{-4}, and CO_2^{-3} ions on goethite, *J. Colloid Interface Sci.*, *320*(2), 400–414.
Stahl, M. O., C. F. Harvey, A. van Geen, J. Sun, P. Thi Kim Trang, V. Mai Lan, T. Mai Phuong, P. Hung Viet, and B. C. Bostick (2016), River bank geomorphology controls groundwater arsenic concentrations in aquifers adjacent to the Red River, Hanoi Vietnam, *Water Resour. Res.*, *52*, 6321–6334, doi:10.1002/2016WR018891.
Stollenwerk, K. (2003), Geochemical processes controlling transport of arsenic in groundwater: A review of adsorption, in *Arsenic in Ground Water*, edited by A. Welch and K. Stollenwerk, pp. 67–100, Springer, New York.
Stollenwerk, K., G. N. Breit, A. H. Welch, J. C. Yount, J. W. Whitney, A. L. Foster, M. N. Uddin, R. K. Majumder, and N. Ahmed (2007), Arsenic attenuation by oxidized aquifer sediments in Bangladesh, *Sci. Total Environ.*, *379*(2–3), 133–150.
Stute, M., et al. (2007), Hydrological control of As concentrations in Bangladesh groundwater, *Water Resour. Res.*, *43*, W09417, doi:10.1029/2005WR004499.
Tessier, A., R. Carignan, B. Dubreuil, and F. Rapin (1989), Partitioning of zinc between the water column and the oxic sediments in lakes, *Geochim. Cosmochim. Acta*, *53*(7), 1511–1522.
Thi Hoa Mai, N., Postma, D., Thi Kim Trang, P., Jessen, S., Hung Viet, P., and Larsen, F. (2014), Adsorption and desorption of arsenic to aquifer sediment on the Red River floodplain at Nam Du, Vietnam, *Geochim. Cosmochim. Acta*, *142*, 587–600.
Tikhonov, A. N., and V. Y. Arsenin (1977), *Solution of Ill-Posed Problems*, 271 pp., Winston, Washington, D. C.
Tournassat, C., L. Charlet, D. Bosbach, and A. Manceau (2002), Arsenic(III) oxidation by birnessite and precipitation of manganese(II) arsenate, *Environ. Sci. Technol.*, *36*(3), 493–500.
van Geen, A., et al. (2013), Retardation of arsenic transport through a Pleistocene aquifer, *Nature*, *501*(7466), 204–207.
Welter, D. E., J. T. White, R. J. Hunt, and J. E. Doherty (2015), Approaches in highly parameterized inversion—PEST++ Version 3, a Parameter ESTimation and uncertainty analysis software suite optimized for large environmental models, *Rep. 7-C12*, 64 pp., Reston, Va.
Winkel, L. H. E., P. T. K. Trang, V. M. Lan, C. Stengel, M. Amini, N. T. Ha, P. H. Viet, and M. Berg (2011), Arsenic pollution of groundwater in Vietnam exacerbated by deep aquifer exploitation for more than a century, *Proc. Natl. Acad. Sci. U. S. A.*, *108*(4), 1246–1251.

Wu, Y., W. Li, and D. L. Sparks (2015), The effects of iron(II) on the kinetics of arsenic oxidation and sorption on manganese oxides, *J. Colloid Interface Sci.*, *457*, 319–328.

Yeh, W. W. G. (1986), Review of parameter identification procedures in groundwater hydrology: The inverse problem, *Water Resour. Res.*, *22*(2), 95–108.

Ying, S. C., B. D. Kocar, S. D. Griffis, and S. Fendorf (2011), Competitive microbially and Mn oxide mediated redox processes controlling arsenic speciation and partitioning, *Environ. Sci. Technol.*, *45*(13), 5572–5579.

Zhang, H., and H. M. Selim (2005), Kinetics of arsenate adsorption−desorption in soils, *Environ. Sci. Technol.*, *39*(16), 6101–6108.